

Chitosan Graft Copolymers-HA/DBM Biocomposites: Preparation, Characterization, and *In Vitro* Evaluation

Khaled R. Mohamed, Gehan T. El-Bassyouni, Hanan H. Beherei

Biomaterials Department, National Research Centre, Dokki, Giza, Egypt

Received 13 August 2006; accepted 10 November 2006

DOI 10.1002/app.26508

Published online 11 May 2007 in Wiley InterScience (www.interscience.wiley.com).

ABSTRACT: The combination of biopolymer with a bioactive component takes advantage of the osteoconductivity and osteoinductivity properties. The studies on composites containing hydroxyapatite (HA), demineralized bone matrix (DBM) fillers and chitosan biopolymer are still conducted. In the present study, the bioactive fillers were loaded onto p(HEMA-MMA) grafted chitosan copolymer to produce a novel biocomposites having osteoinductive and osteoconductive properties. The produced composites were assessed by TGA, XRD, FTIR, and SEM techniques to prove the interaction between both matrices. *In vitro* behavior of these composites was performed in SBF to verify the

formation of apatite layer onto their surfaces and its enhancement. The results confirmed the formation of thick apatite layer containing carbonate ions onto the surface of biocomposites especially these containing HA-DBM mixture and pMMA having bone cement formation in their structure. These a novel biocomposites have unique bioactivity properties can be applied in bone implants and tissue engineering applications as scaffolds in future. © 2007 Wiley Periodicals, Inc. *J Appl Polym Sci* 105: 2553–2563, 2007

Key words: biopolymer; graft copolymer; fillers; FTIR; implant

INTRODUCTION

Chitosan was suggested as an alternative polymer for use in orthopedic applications to provide mechanical support and the regeneration of bone cell ingrowths.¹ Chitosan is biocompatible, biodegradable, non toxic, improves osseous healing, and stimulates cell proliferation.² Poly hydroxyethylmethacrylate (pHEMA) has potentially wide biomedical applications because it is biocompatible, allows immobilization of cells or bioactive molecules and has hardness comparable to bone.³ Among the many potential bone cement materials, pMMA or its derivatives have been used successfully in orthopedic surgeries. pMMA conforms to the shape of its surroundings and forms a strong mechanical bond with implants. Modified pMMA can be made by adding hydroxyapatite (HAp) powder that is highly reactive and favorable for attachment and bioactivity.⁴ The use of chitosan-based copolymers and the use of hydroxyethylmethacrylate (HEMA) as a grafting monomer onto range of polymeric substrates provide materials with desired properties. These copolymers improve the biocompatibility of the calcium phosphates, which increase its use as biomaterials.⁵ Increasing the mechanical properties and the bioactivity of surgical cement, the linkage of two mono-

mers, HEMA and MMA, by copolymerization to a modified apatite was reported.⁶

HA and DBM are generally used as bone substitutes in orthopedic, oral, and maxillofacial surgery. HA has similar chemical composition and structure to the mineral phase of human bone.⁷ Calcium phosphate ceramics possess osteoconductive properties, but they do not have intrinsic osteoinductive capacity and they are unable to induce new bone formation in extra-osseous sites.⁸ DBM is allograft bone from which the mineral portion has been removed and is effective as a bone graft extender in an animal model.⁹ Also, DBM possesses osteoconductivity as well as osteoinductivity properties.¹⁰

In the past few years, increasing attention has been paid to composites made of polymers and ceramics for application in tissue engineering composites scaffolds which may prove necessary for reconstruction of multi-tissue organs, tissues interfaces and structural tissue including bone, cartilage, tendons, ligaments, and muscles. Composite fabrication research has focused on developing polymer/ceramics blends, precipitating ceramic onto polymer templates and coating polymers onto ceramic or ceramic onto polymers.¹¹ An important factor which reduces new bone formation is the difficulty of mixing HA granules with DBM pieces evenly. When DBM was implanted with HA, a large amount of BMP from DBM diffused directly to host tissues around the DBM pieces rather than passing into the pores of HA granules, then fibrous tissue is initiated

Correspondence to: K. R. Mohamed (kh_rezk@yahoo.com).

by HA granules which is the main factor interfering with osteoinduction.¹⁰ Thus, using glycerol or fibrin to glue HA with DBM pieces or BMP was prepared for more favorable bone induction.¹² Incorporation of HAp, the mineral component of bone with chitosan, could improve the bioactivity and the bone bonding ability of the chitosan/HAp composites.¹³ Chitosan just plays a role of adhesive to dissolve the problem of difficulty of calcium phosphate powder specific shape and migration of particles when implanted.¹⁴

The potential bioactivity of the material being evaluated by *in vitro* studies is much cheaper and quicker than *in vivo* studies. Besides, they are useful in both designing new biomaterials and improving the existing material for better bioactivity. From this point of view, in the present study, a novel biocomposites containing HA, DBM, and chitosan grafted with p(HEMA-MMA) copolymer matrix were fabricated and characterized using different techniques to assess the homogeneity within the composite. Also, these biocomposites were followed in SBF to assess the bioactivity behavior and to confirm the formation of apatite layer onto their surfaces and its enhancement.

MATERIALS AND METHODS

Materials

Chitosan polymer ($C_6H_{11}NO_4$), HEMA ($CH_2=CCH_3COO C_2 H_4OH$) and MMA ($H_2C=C(CH_3)CO_2CH_3$) monomers were provided from Aldrich. Ceric ammonium nitrate initiator (CAN) ($(NH_4)_2 [Ce (NO_3)_6]$) was provided from (BDH, UK). HA of size 150 μm was provided from Sigma and demineralized bone matrix powder (DBM) having particle size 150 μm was prepared according to (Abed Fattah and El-Bas-syouni).¹⁵ HA/DBM filler powder (Particle size: 150 μm) was prepared via well mixing of 0.75 g of HA powder with 0.75 g of DBM powder (50:50% in weight).

Method

Preparation of HA and HA-DBM composites I

Chitosan (0.1g) was dissolved in 7.5 mL of 3% acetic acid solution then 2.5 mL of HEMA monomer (total volume = 10 mL) and 0.1 g CAN as an initiator were added and well mixed to graft the monomer onto chitosan polymer surface. The copolymer mixtures were kept in water bath at 40°C for 2.5 h to nearly achieve the copolymerization process. Fixed weight (1.5 g) from each filler HA and HA-DBM was well dispersed and mixed into the copolymer mixture and kept at 40°C in water bath for 30 min later to complete the copolymerization in the presence of the filler powder. The two copolymer/filler

mixtures were left overnight at room temperature and then washed with hot ethanol with stirring for 1 h to remove homopolymer. Both mixtures was filtered, collected, and dried at 60°C for 24 h. The grafting (G%) in the presence of filler is calculated according to the following equation.¹⁶

$$G(\%) = (g - g_0/g_0) \times 100$$

where g is weight of the grafted chitosan in the presence of filler and g_0 is weight of the original chitosan. The obtained HA/and HA-DBM/chitosan composites by pHEMA copolymer matrix were denoted as HA/chitosan composite I and HA-DBM/chitosan composite I, respectively.

Preparation of HA and HA-DBM composites II

Chitosan (0.1 g) was dissolved in 7.0 mL of 3% acetic acid solution then 2.5 mL of HEMA, 0.5 mL MMA monomers (total volume = 10 mL), and 0.1 g CAN were added and well mixed to graft the monomer onto chitosan polymer surface. The copolymer mixtures were put in water bath at 40°C for 2.5 h to nearly achieve the copolymerization process. Fixed weight (1.5 g) from each filler HA and HA-DBM was well dispersed into the copolymer mixture and kept at 40°C in water bath for 30 min later to complete the copolymerization in the presence of the filler powder. The two copolymer/filler mixtures were left overnight at room temperature and then washed with ethanol-acetone mixture with stirring for 1 h to remove homopolymer. Both mixtures was filtered, collected, and dried at 60°C for 24 h. The grafting (G%) in the presence of filler is calculated according to the previous equation. The obtained HA/and HA-DBM/chitosan composites pHEMA-MMA copolymer matrix were denoted as HA/chitosan composite II and HA-DBM/chitosan composite II, respectively.

Characterization

The thermal properties of starting fillers and their composites were evaluated by thermogravimetric analysis (TGA) using a Perkin-Elmer, 7 series thermal analyzer in nitrogen atmosphere at a heating rate of 10°C/min over the temperature range of 50–1000°C. The phase analysis of samples was examined by X-Ray diffractometer (Diana Corporation, USA) equipped with CoK_{α} radiation, $\lambda = 1.79026 \text{ \AA}$ (with Fe filter). The FTIR spectra were measured using KBr pellets made from a mixture of powder for each sample and were assessed from 400 to 4000 cm^{-1} using a Nexus 670, Nicloet FTIR spectrometer, USA. Scanning electron microscopy (SEM), JXA 840A Electron Probe Microanalyzer (JEOL, Japan). For SEM,

TABLE I
The Grafting (%) and Weight Loss (%) of the Prepared Composites

	HA/chitosan composite I	HA/chitosan composite II	HA-DBM/chitosan composite I	HA-DBM/chitosan composite II
G (%)	2254	2411	2514	2654
Weight loss(%)	33.30	37.64	57.73	71.43

the substrates were mounted on metal stubs and coated with gold before being examined.

Testing

Mechanical. The composites were tested to determine the effect of filler on mechanical properties. The compressive strength was measured using tensile testing machine, Zwick Z010, Germany. The average value for each test was taken for three samples to confirm the results.

Biodegradation test. The biodegradation study of the composites was carried out *in vitro* by incubating the composite in SBF at pH: 7.4 and 37°C for different periods. At interval time, the composites were taken from the medium, washed with distilled water and dried at 60°C overnight. The degradable ratio (D) was examined by weight loss from the following formula:

$$D = (W_0 - W_t)/W_0 \times 100$$

where W_0 denotes the original weight, while W_t is the weight at time t . Each experiment was carried out for 3 samples and the average value was taken to confirm the results.¹⁷

Water absorption ability. Water absorption (W.A %) studies are of great importance for a biodegradable material. For water-uptake measurements, all the specimens were weighed before being immersed in distilled water. After immersion for different periods, the samples were carefully removed from the medium and immediately weighed for the determi-

nation of the wet weight as a function of the immersion time.¹⁸ Water absorption is given using the following equation.

$$W.A = [(W_f - W_i)/W_i] \times 100$$

where W_i is the initial weight of the sample, and W_f is the sample weight after soaked time of immersion. The experiment was carried out for 3 samples and the average value was taken to ensure the results.

In vitro test. To study the bioactivity, the samples were soaked in SBF, proposed by Kokubo and Takadama,¹⁹ at body temperature (37°C) and pH = 7.4 for several periods up to 8 days. The SBF has a composition similar to human blood plasma and has been extensively used for *in vitro* bioactivity tests. After the immersion periods end, the solutions were analyzed by spectrophotometer (UV-2401PC, UV-VIS, Recording spectrophotometer, Shimadzu, Japan) using biochemical kits (Techo Diagnostic, USA) to detect the total calcium ions (Ca^{2+}) at $\lambda = 570$ nm and phosphate ions (PO_4^{3-}) concentration at $\lambda = 675$ nm. Each test was carried out for 3 samples and the average value was taken to ensure the results. The specimens immersed were removed from the SBF solution then abundantly rinsed using deionized water and dried to complete the required investigation.

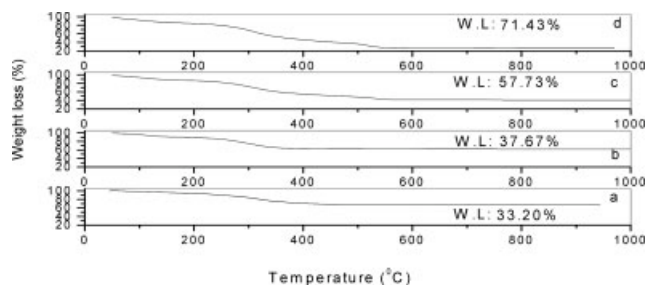


Figure 1 TGA analyses of (a) HA/chitosan composite I, (b) HA/chitosan composite II, (c) HA-DBM/chitosan composite I and (d) HA-DBM/chitosan composite II.

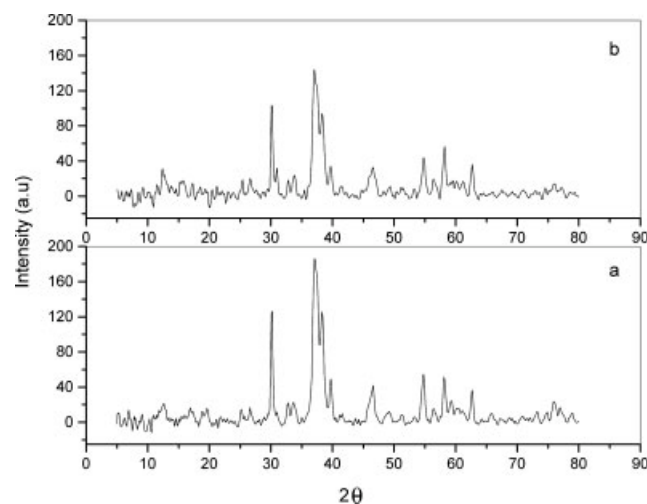


Figure 2 XRD patterns of (a) HA powder and (b) HA-DBM powder.

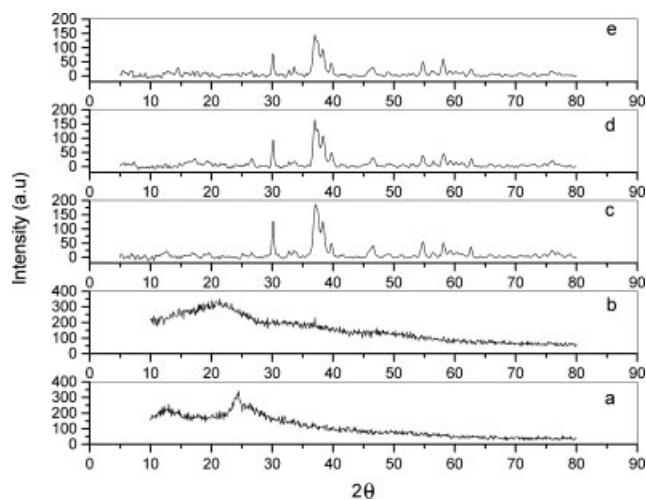


Figure 3 XRD patterns of (a) chitosan, (b) copolymer, (c) HA filler, (d) HA/chitosan composite I and (e) HA/chitosan composite II.

RESULTS AND DISCUSSION

The grafting % and TGA analysis

Table I shows the grafting % and weight loss of the prepared composites. The presence of HA-DBM filler particles into the copolymer matrix containing the grafted chitosan by pHEMA and by p(HEMA-MMA) enhanced the grafting % as in HA-DBM/chitosan composite I and II (2514 and 2654%), respectively, compared with HA/chitosan composite I and II (2254 and 2411%), respectively. This result proved that the presence of DBM powder into HA/copolymer composite enhanced the grafting % because of the amorphous structure of DBM filler¹⁵ resulting in high penetration within the copolymer matrix and

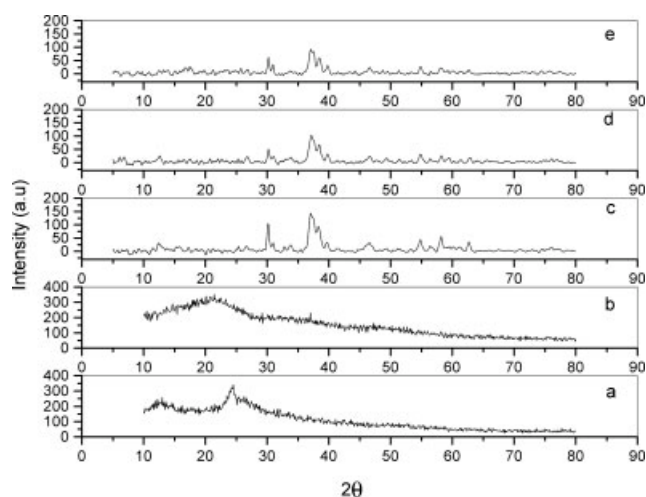


Figure 4 XRD patterns of (a) chitosan, (b) copolymer, (c) HA-DBM filler, (d) HA-DBM/chitosan composite I and (e) HA-DBM/chitosan composite II.

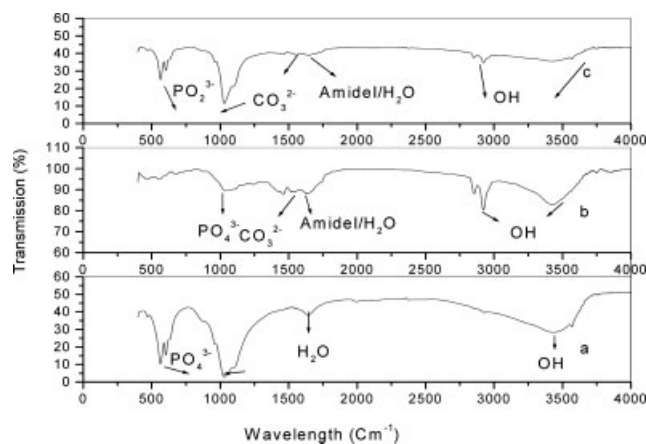


Figure 5 FTIR of (a) HA powder, (b) DBM powder, and (c) HA-DBM filler powder.

do not inhibit the effect of free radicals to increase the grafting %. The TGA analysis show that the same composites HA-DBM/chitosan composites I and II containing DBM powder in its structure having the highest G% (2514 and 2654%) had also the highest weight loss 57.73 and 71.43% accompanying the evolution of all NH_3 , CO_2 , and H_2O ,²⁰ respectively, confirming high affinity of HA-DBM powder to the copolymer (Fig. 1). The grafting % and TGA results confirmed that the composite containing filler into the pHEMA-MMA copolymer matrix (as in HA-DBM/chitosan composite II) had enhanced the attached copolymer onto the particles surface of filler proving high affinity of DBM powder to the copolymer due to its amorphous structure. This result proved the role of pMMA which enhanced the grafting % of this composite compared to HA-DBM/chitosan composite I.

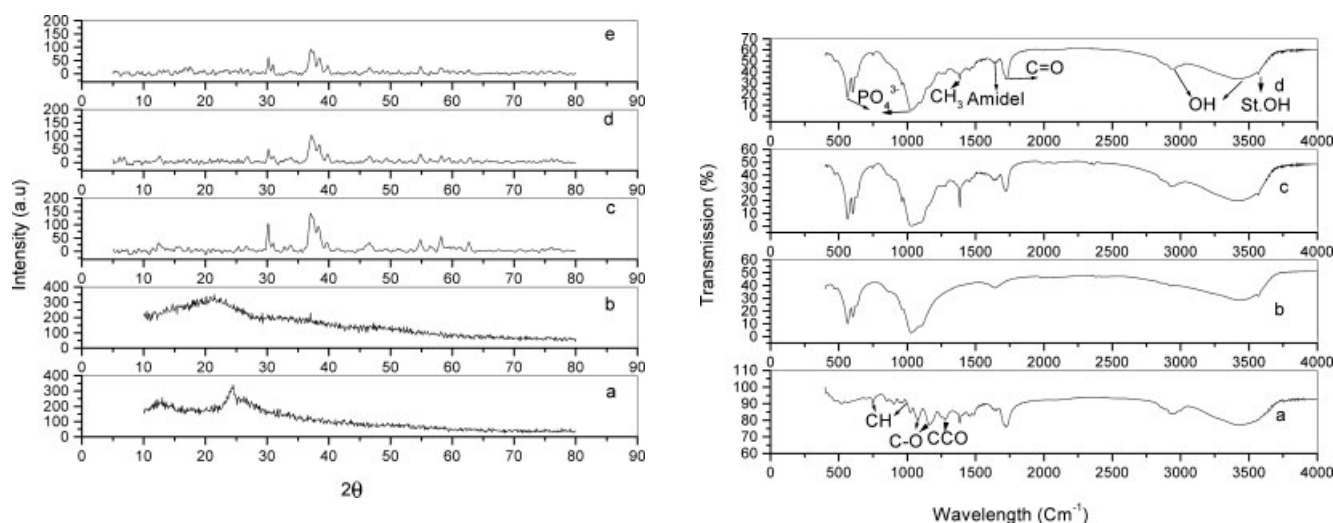


Figure 6 FTIR of (a) copolymer (b) HA powder, (c) HA/chitosan composite I and, (d) HA/chitosan composite II.

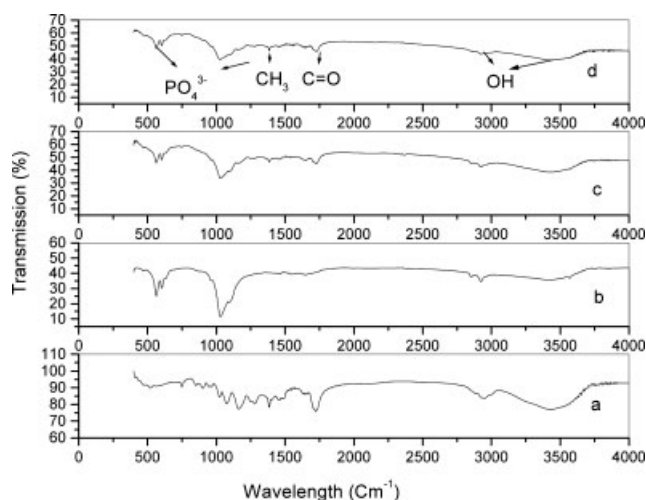


Figure 7 FTIR of (a) copolymer (b) HA-DBM powder, (c) HA-DBM/chitosan composite I, and (d) HA-DBM/chitosan composite II.

Characterization

Phase analysis

Figure 2 shows the patterns of HA powder and HA-DBM powder. The peaks intensity of HA powder reduced after addition of DBM powder to HA filler (Card No. 74-0565) due to amorphous structure of DBM powder. Figures 3(b) and 4(b) show the XRD patterns of copolymer which proves the formation of copolymer via the grafting of HEMA and MMA monomers onto chitosan polymer surface. The patterns of chitosan into the copolymer structure are broad and appear at d -spacing = 2.86, 4.75, and 5.52 with lower intensity and some shift to lower angle compared to the original chitosan (Card No: 39-1894) [Figs. 3(a) and 4(a)] proving chemical interaction between chitosan polymer and monomers.²¹ The XRD patterns of HA/chitosan composites I and II show that the peaks of HA have lower intensity compared to HA filler proving effect of coating especially HA/chitosan composite II containing mixture of pHEMA-MMA copolymer (Fig. 3). The patterns of HA-DBM/chitosan composites I and II show that the peaks of HA have lower intensity compared to HA-DBM filler proving effect of coating especially HA-DBM/chitosan composite II containing mixture of pHEMA-MMA copolymer. This result confirmed that the HA-DBM composite containing in its structure chitosan grafted by p(HEMA-MMA) copolymer

matrix had the highest coating onto the particles surface and coincided with the grafting and TGA data due to the importance of the role pMMA⁴ and DBM powder to obtain the composite having a suitable properties.

FTIR analysis

Figure 5 shows FTIR of HA, DBM, and HA-DBM fillers. Characteristic groups of HA and DBM such as OH of water molecules, amide I, carbonate, and phosphate bands still exist in HA-DBM spectrum and their O.D values were reduced compared to original HA and DBM proving that each fillers has an effect on the other. Figure 6 shows FTIR of copolymer, HA powder, HA/chitosan composites I and II. The bands of HA in two composites I and II spectra appeared at 3570, 3431, 1029, 630, and 603–564 cm^{-1} which were assigned to stretching OH, OH of water, stretching phosphate, librational OH, and bending phosphate, respectively.²² These bands are still present after loading of HA filler into the copolymer and their O.D were reduced compared to original HA proving effect of coating on these sites especially HA/chitosan composite II containing the increased % of the grafted copolymer. Figure 7 shows that the characteristic bands for HA-DBM filler in two composites I and II spectra. These bands are still present after loading of HA-DBM filler onto the copolymer matrix and their O.D values were reduced compared to original HA-DBM powder proving effect of coating on these sites especially HA-DBM/chitosan composite II due to high content of the formed copolymer which attached to the filler particles. This result is coinciding with the results of the G%, TGA, XRD which recorded the highest values for HA-DBM/chitosan composite II due to high content of monomers for copolymerization process and surface chemistry of HA-DBM powder.

Testing

Mechanical

Table II shows the mechanical properties of HA/chitosan composites I and II and HA-DBM/chitosan composites I and II. The E-modulus and compressive strength for HA-DBM/chitosan composite II recorded lower values compared to other composites. In this context, therefore, the presence of HA-DBM

TABLE II
The Mechanical Properties of the Prepared Composites

	HA/chitosan composite I	HA/chitosan composite II	HA-DBM/chitosan composite I	HA-DBM/chitosan composite II
E-Modulus (N/mm^2)	672.86	563.68	632.62	377.12
Compressive strength (MPa)	20.30	20.28	22.50	12.12

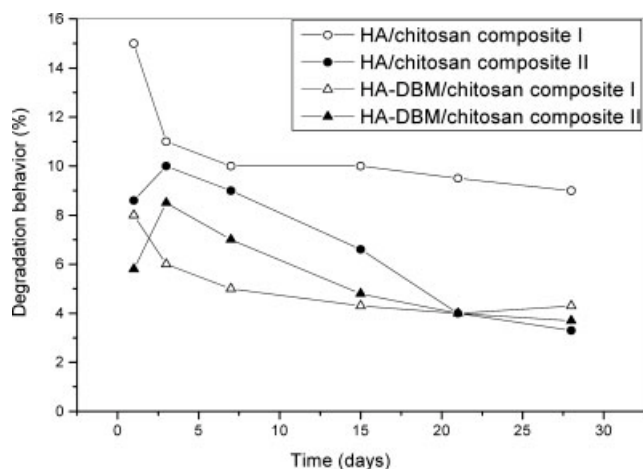


Figure 8 Biodegradation test (%) of HA and HA-DBM fillers/chitosan composites.

filler into p(HEMA-MMA) grafted chitosan copolymer matrix resulted in compressive strength properties are quite close to those of cancellous bone (2–12 MPa) Kokkubo et al.²³ This result is due to effect of the presence of DBM powder and pMMA having bone cement formation⁴ within this composite.

Biodegradation test

The biodegradation behavior of HA/and HA-DBM/chitosan composites I and II in SBF for various periods was investigated. The weight loss (%) of composite as a function of degradation time is illustrated in Figure 8. The rate of degradation behavior (weight loss) of HA-DBM/chitosan composites I and II was significantly slower than that of HA/chitosan composites I and II at all periods proving the stability of these composites which contain DBM powder into their structure. This result is due to high attachment

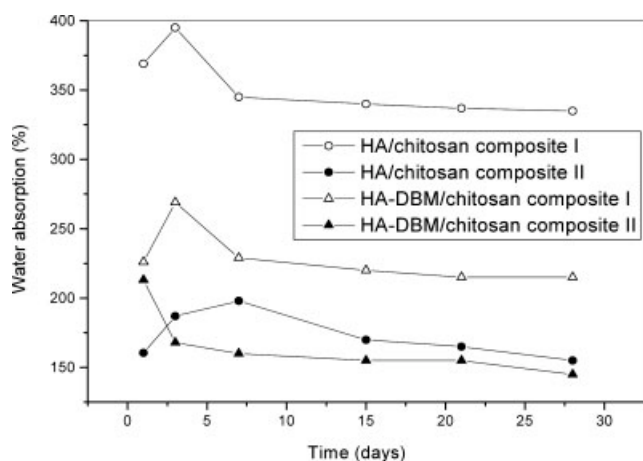


Figure 9 Water absorption (%) of HA and HA-DBM fillers/chitosan composites.

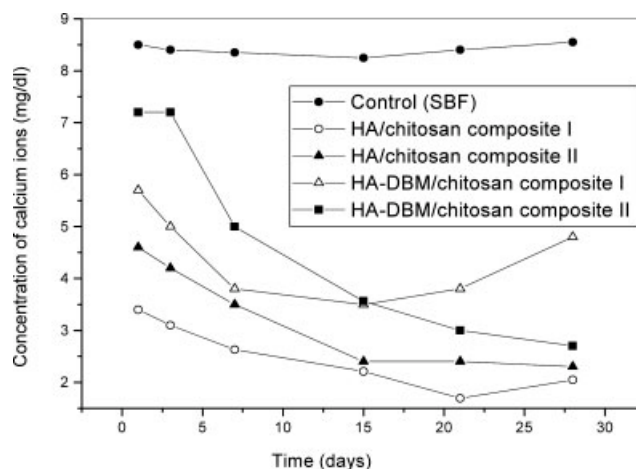


Figure 10 Concentration of Ca^{2+} ions in SBF postimmersion of fillers chitosan composites compared to control.

of copolymer matrix to DBM particles characterizing amorphous structure and contains bone morphogenetic proteins (BMPs).²⁴

Water absorption test

Figure 9 shows the W.A% of the prepared composites which recorded higher values for HA and HA-DBM/chitosan composites I compared to HA and HA-DBM/chitosan composites II especially HA/chitosan composite I at all time intervals proving higher affinity of composite to water molecules due to the presence of pHEMA grafted containing plentiful hydrophilic groups on its surface. This result proved that HA/and HA-DBM/chitosan composites II having lower W.A % due to the presence of pMMA copolymer part characterizing hydrophobicity properties in these composites as well as the formation of a temporary HA-DBM filler barrier preventing water

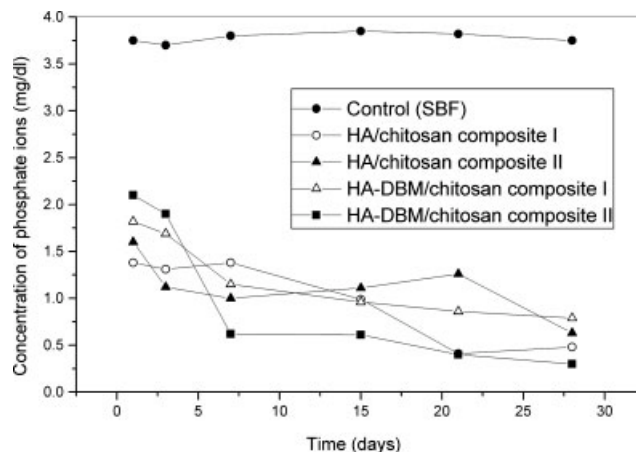


Figure 11 Concentration of phosphate ions in SBF postimmersion of fillers chitosan composites compared to control.

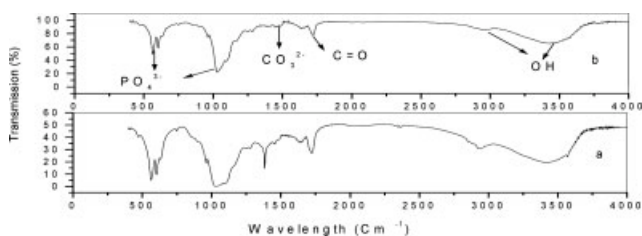


Figure 12 FTIR of HA/chitosan composite I (a) pre- and (b) postimmersion in SBF for 21 days.

permeating into chitosan matrix²⁵ leading to the stability of composite.

In vitro test

Calcium and phosphate ions were measured in SBF after withdrawal of the composite samples from SBF for different periods to assess the ability of the material for the deposition of these ions or their release into the media.

Total calcium ions. Figure 10 shows concentration of Ca^{2+} ions in SBF post immersion of HA, HA-DBM fillers, and their composites with copolymer for different periods compared to control (SBF). Concentration of Ca^{2+} ions recorded lower values for all composites compared to control especially after longer time proving deposition of Ca^{2+} ions onto the composite surface due to the presence of copolymer within the filler particles. Gaillard et al. reported that calcium phosphate formed either on or underneath the surface of copolymer depending on the pH of solution.²⁶ This result proves that HA/or HA-DBM/chitosan composites have enhanced deposition for Ca^{2+} ions especially HA/chitosan composites I and II. Finise et al.²⁷ reported that chitosan forms a water insoluble gel in the presence of calcium ions presenting pharmacologically beneficial effects on osteoconductivity.

Phosphate ions. Figure 11 shows concentration of PO_4^{3-} ions in SBF post immersion of HA, HA-DBM fillers, and their composites with copolymer for different periods compared to control (SBF). Concentration of ions postimmersion recorded lower values for all composites compared to control especially af-

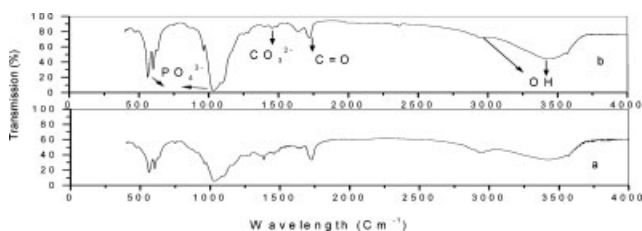


Figure 13 FTIR of HA/chitosan composite II (a) pre- and (b) postimmersion in SBF for 21 days.

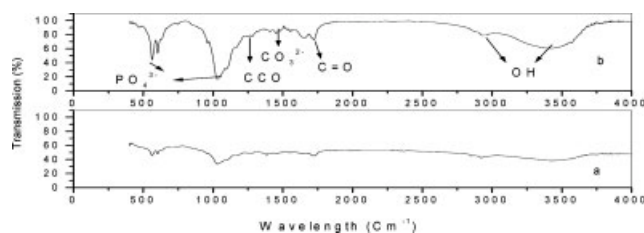


Figure 14 FTIR of HA-DBM/chitosan composite I (a) pre- and (b) postimmersion in SBF for 21 days.

ter longer time proving deposition of PO_4^{3-} ions onto the composite surface because of the presence of copolymer within the filler leads to the deposition of PO_4^{3-} ions. In this context, this could be due to the affinity of chitosan into the copolymer as cationic polymer to phosphate groups as reported by Wang et al.²⁸ So, we could expect the occurrence of interaction between phosphate ions in SBF and amino groups of chitosan into the composite especially HA-DBM/chitosan composite II, therefore, the presence of copolymer into the filler enhanced the ability to promote the formation of calcium phosphate layer.

Solid characterization

The solid bio-composites were investigated postimmersion for 21 days after their withdrawal from SBF by FTIR and SEM-EDAX to confirm the formation of apatite layer onto the surface of composites.

FTIR assessment

FTIR of HA/chitosan composites (I and II) and HA-DBM/chitosan composites (I and II) preand postimmersion in SBF for 21 days are shown in (Figs. 12–15). All bands characterizing HA, DBM, and copolymer structure in the composites spectra appeared at 3570, 3420, 2920, 1720, 1640, 1280, 1030–960, 630, 602–560 cm^{-1} and were assigned to stretching of OH, OH of water, OH and CH, C=O, absorbed water/amide I, CCO, stretching PO_4^{3-} , librational OH and bending PO_4^{3-} groups, respectively.²⁹ These bands appeared postimmersion and their O.D values were reduced compared to preim-

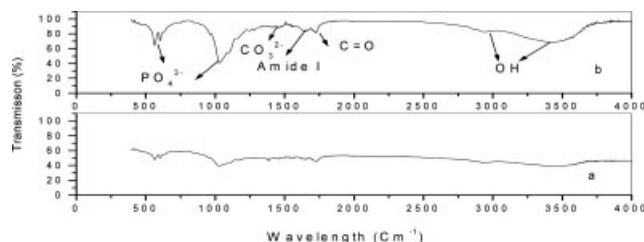


Figure 15 FTIR of HA-DBM/chitosan composite II (a) pre- and (b) postimmersion in SBF for 21 days.

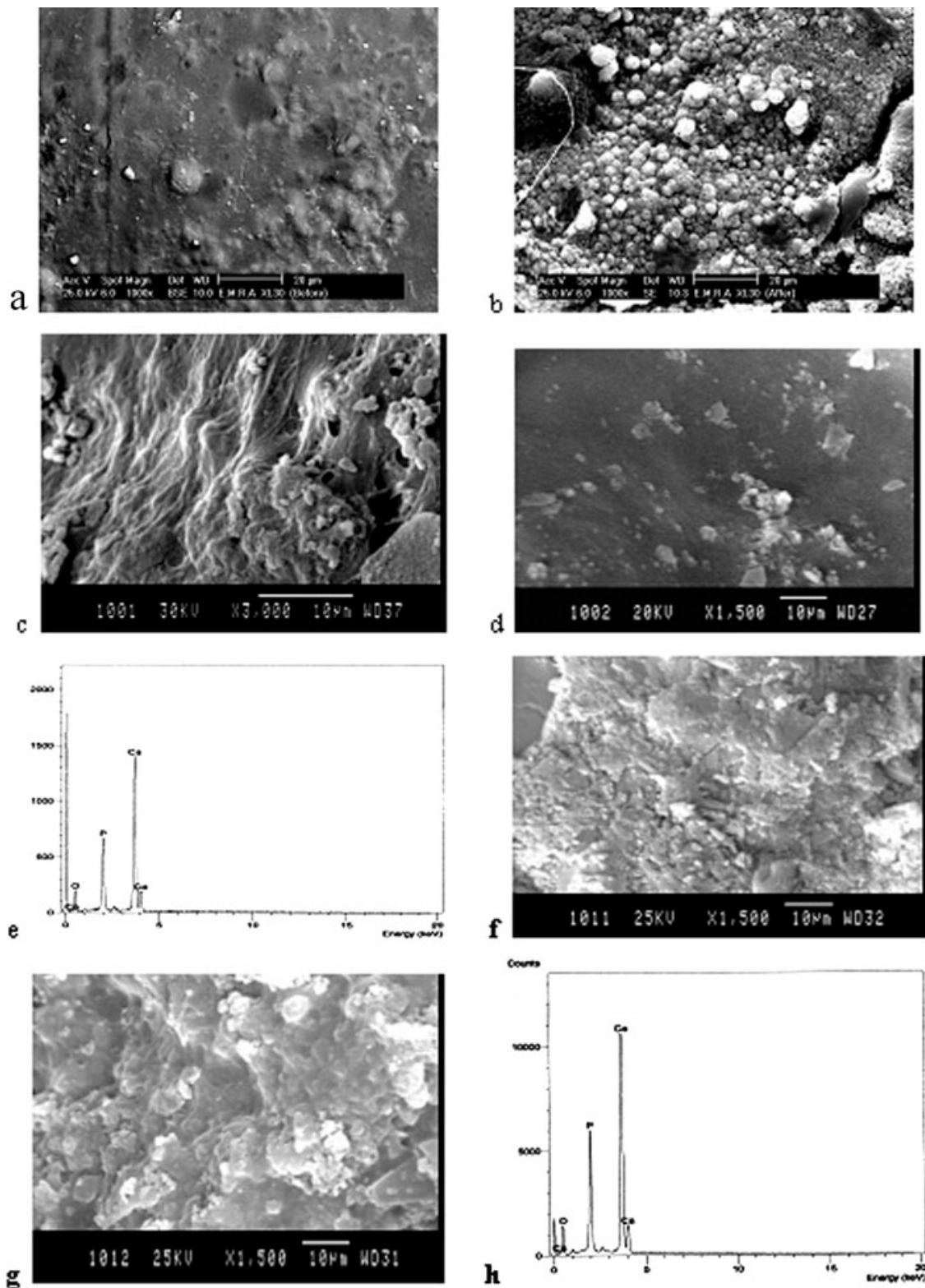


Figure 16 SEM of copolymer (a) pre- and (b) postimmersion, HA/chitosan composite I (c) pre-, (d) postimmersion, and (e) its EDAX analysis and HA/chitosan composite II (f) pre-, (g) postimmersion, and (h) its EDAX analysis.

mersion proving effect of immersion and its involvement in the composite surface except the band at 1030 cm^{-1} in HA/chitosan composite II and HA-DBM/chitosan composite I. This band at 1030 cm^{-1}

which is assigned to stretching phosphate had enhanced O.D values in HA/chitosan composite II and HA-DBM/chitosan composite I postimmersion compared to preimmersion denoting deposition of

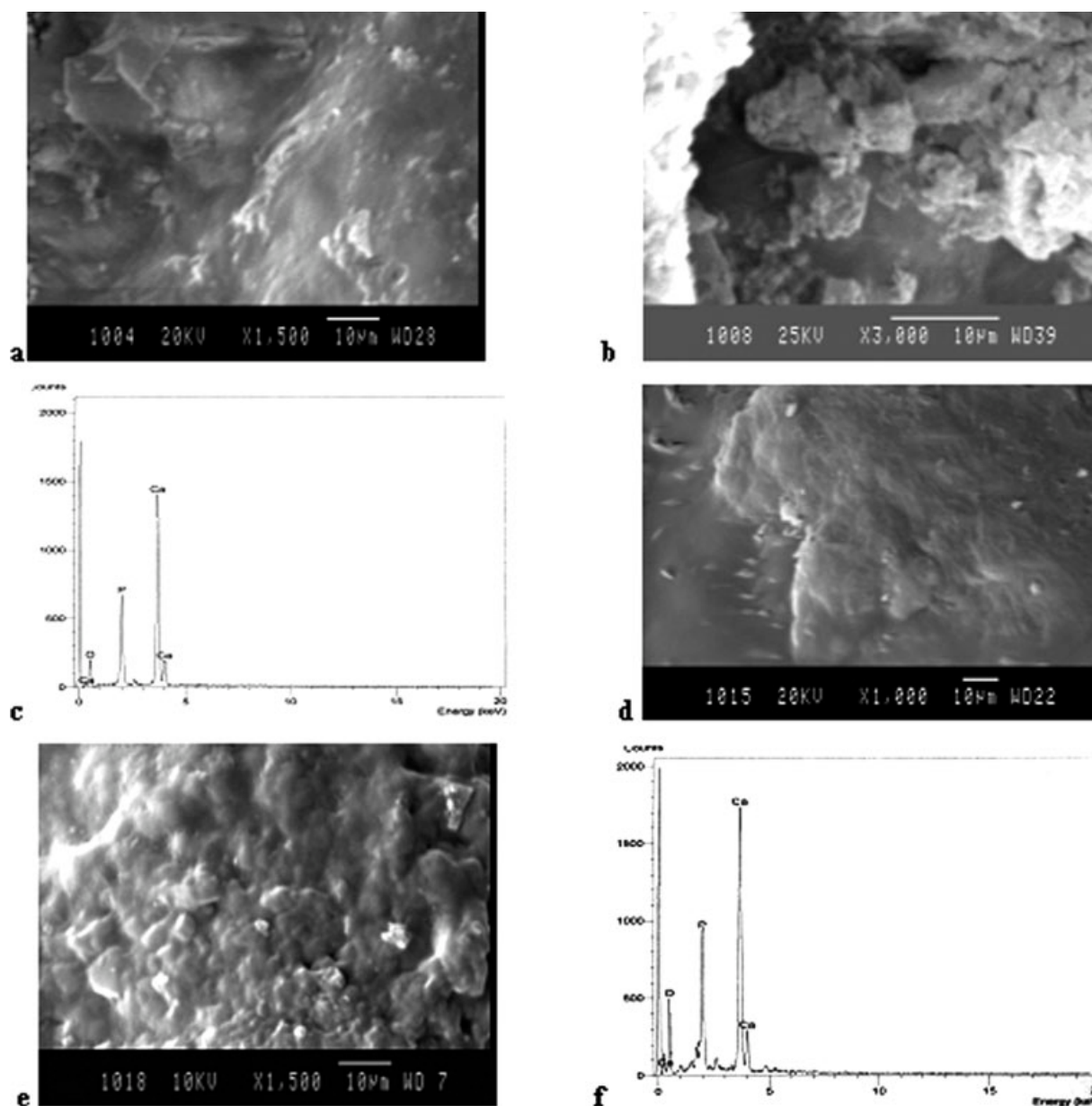


Figure 17 SEM of HA-DBM/chitosan composite I (a) pre-, (b) postimmersion, and (c) its EDAX analysis and HA-DBM/chitosan composite II (d) pre-, (e) postimmersion, and (f) its EDAX analysis.

phosphate ions on the composite surface, this result is in favor of the formation of apatite layer. Also, new band appeared at 1450 cm^{-1} assigned to carbonate group postimmersion in SBF for HA/chitosan composites I and II, therefore, these composites had ability to form the carbonated apatite layer. In this domain, carbonate ions play a vital role in the bone metabolism and they occupy about 3–8% weight of the calcified tissue, therefore, the carbonate substituted HAP may have a tremendous potential in bone-related therapy.³⁰ Also, the same carbonate group reappeared postimmersion in HA-DBM/chitosan composites I and II denoting also formation of carbonated apatite layer.

Surface morphology

The copolymer and HA/chitosan composites I and II. For copolymer preimmersion [Fig. 16(a)], SEM shows smooth surface with coated particles proving formation of copolymer matrix. On the other hand, postimmersion, Figure 16(b) indicates the appearance of plentiful spherical particles on the copolymer surface proving formation of apatite layer. Therefore, we can expect that the presence of copolymer within the filler particles will lead to the enhancement of apatite formation onto the composite surface Figure 16(c) shows SEM of HA/chitosan composite I preimmersion in SBF for 21 days. It indicates the presence of smooth surface with bright longitudinal lines and

some pores as well as HA particles deposited onto the surface proving coating and integration within the composite. Fine particles of HA are found to aggregate and precipitate into the copolymer matrix. One of the possible reasons may be due to the fact that some of the HA particles might have partially dissolved in the acidic copolymer solution that makes HA particles to penetrate easily into the copolymer matrix. The particles of composite showed a high tendency to agglomerate and hence it acquires capability to prevent the particle mobilization postimplantation. While postimmersion, Figure 16(d) shows the presence of many small and large particles (hexagonal shape) with bright color denoting deposition of calcium phosphate particles and its Ca/P ratio recorded 2.09 which determined by EDAX analysis [Fig. 16(e)]. Figure 16(f) shows SEM of HA/chitosan composite II preimmersion, the presence of HA particles connected to each other via the copolymer proving integration and homogeneity within the composite. Postimmersion, Figure 16(g) shows the appearance of bright spherical particles and some nodules as well as few pores indicating effect of immersion and growth of apatite layer and its Ca/P ratio recorded 1.8 which is near from standard Ca/P ratio (1.67) to form HA apatite [Fig. 16(h)]. *HA-DBM/chitosan composites I and II*. Figure 17a shows SEM of HA-DBM/chitosan composite I preimmersion in SBF for 21 days. It indicates the presence of smooth surface with some deposited bright particles onto the surface proving high coating, homogeneity and integration within the composite. Postimmersion, Figure 17(b) shows the presence of plentiful aggregated particles with bright color denoting high deposition of calcium phosphate particles onto the surface and its Ca/P ratio recorded 2.02 [Fig. 17(c)]. SEM of HA-DBM/chitosan composite II preimmersion, Figure 17(d) shows the appearance of smooth surface with some minute particles onto the surface proving high coating and homogeneity. Postimmersion, Figure 17(e) shows the appearance of bright spherical particles and nodules with some swelling of copolymer part indicating effect of immersion and growth of apatite layer as well as Ca/P ratio recorded 1.65 which is very close to standard Ca/P ratio (1.67) for the formation of HA [Fig. 17(f)]. This result proved the presence of the copolymer matrix containing chitosan polymer grafted with mixture from HEMA-MMA monomers resulted in the formation of a bone-like apatite layer having Ca/P ratio very close to the standard ratio in bone, this is due to the presence of pMMA characterizing the formation of bone cement in the composite structure.⁴

Finally, it is notified that these results coincide with the results of *in vitro* test and FTIR proving the presence of copolymer into the HA or HA-DBM bio-

composites leading to the precipitation of calcium phosphate (apatite layer) onto the surface especially HA and HA-DBM/chitosan composites II.

CONCLUSIONS

The grafting, TGA, XRD, and FTIR results confirmed that the prepared composites containing HA-DBM mixture powder into the copolymer matrix containing the grafted chitosan with methylmethacrylate (pMMA) and its derivative (pHEMA) had enhanced the coating and attached copolymer onto the surface particles. Water absorption properties had enhanced for HA/chitosan composite I containing pHEMA characterizing hydrophilicity properties in its structure proving its lower stability into the media (SBF) while HA and HA-DBM/chitosan composites II were more stable because of the hydrophobicity of pMMA properties. It is notified that the results of *in vitro* test, FTIR and SEM provided by elemental analysis (EDAX) postimmersion confirmed that the presence of HA or HA-DBM filler particles within copolymer matrix especially and HA and HA-DBM/chitosan composites II having pMMA characterizing bone cement properties in their structure leads to the enhancement of formation of carbonated apatite layer having Ca/P ratio very close to the standard in the bone (1.67) onto their surfaces. Finally, novel bio-composites have unique bioactivity properties can be applied in bone defects and tissue engineering applications as scaffolds in future.

References

- Vande Vord, P. J.; Matthew, H. W. T.; Desilua, S. P.; Mayton, L.; Wu, B.; Wooley, P. H. *J Biomed Mater Res* 2002, 59, 585.
- Mohamed, K. R.; El-Meliegy, E. *Ceramics International*, 2006 (in press).
- Filmon, R.; Grizon, F.; Baslé, M. F.; Chappard, D. *J Biomat* 2002, 23, 3053.
- Kima, S. B.; Kima, Y. J.; Yoonb, T. L.; Parka, S. A.; Choa, I. H.; Kima, E. J.; Kima, I. A.; Shina, J. *Biomaterial* 2004, 25, 5715.
- Casimiro, M. H.; Betelho, M. L.; Leal, J. P.; Gil, M. H. *Rad Phys Chem* 2005, 72, 731.
- Delpuch, V.; Lebugle, A. *Clin Mater* 1990, 5, 209.
- Sato, M.; Slamovich, E. B.; Webster, T. J. *J. Biomaterials* 2005, 26, 1349.
- Kastena, P.; Luginbuhl, R.; van Griensven, M.; Barkhausenc, T.; Krettek, C.; Bohner, M.; Bosch, U. *J Biomater* 2003, 24, 2593.
- Marone, M. A.; Boden, S. D. *J Spine* 1998, 23, 159.
- Lindholm, T. C.; Gao, T. J.; Lindholm, T. S. *Annales Chirurgiae et Gynaecologiae* 1993, 82, 91.
- Marquet, V.; Boccaccini, A. R.; Pravata, L.; Notingher, I.; Jerome, R. *Biomaterial* 2004, 25, 4185.
- Sato, T.; Kawamura, M.; Sato, K.; Iwata, H.; Miura, T. *J. Clin Orthop* 1991, 263, 254.
- Wang, X. H.; Ma, J. B.; Wang, Y. N.; He, B. L. *J Biomater* 2002, 23, 4167.
- Qiaoling Hu, Q.; Li, B.; Wang, M.; Shen, J. *J. Biomaterial* 2004, 25, 779.

15. Abdel Fattah, W.; El-Bassyouni, G.; Egypt, J. Biophys Biomed Eng 2002, 3, 175.
16. Singh, D. K.; Ray, A. R. J Carbohydr Polym 1998, 36, 251.
17. Mao, J. S.; Liu, H. F.; Yin, Y. J.; Yao, K. D. J Biomater 2003, 24, 1621.
18. Oliveira, A. L.; Malafaya, P. B.; Reis, R. L. J Biomater 2003, 24, 2575.
19. Kokubo, T.; Takadama, H. J Biomater 2006, 27, 2907.
20. Angelova, N.; Manolova, N.; Rashikov, L. J Bioactive Compatible Polym 1995, 10, 10.
21. Prashanth, K. V. H.; Tharanathan, R. N.; Hu, Q.; Li, B.; Wang, M. S. J Biomater 2004, 25, 779.
22. Chen, F.; Wang, Z.; Lin, C. Mater Lett 2002, 57, 858.
23. Kokubo, T.; Kim, H.; Kawashita, M. J Biomater 2003, 24, 2161.
24. Sandhu, H. S.; Khan, S. N.; Suh, D. Y.; Boden, S. D. J Eur Spine 2001, 10, 122.
25. Hu, R. N.; Li, B.; Shen, W. M. J Biomater 2004, 25, 779.
26. Gaillard, M. L.; Dewijn, I. R.; van Blitterswijk. In Bioceramic, 6 ed.; Christiansen, D.; Ducheyne, Eds.; Elsevier Science, USA, 1993.
27. Finisie, M. R.; Josue, A.; Favere, V. T.; Laranjeira, M. C. An Acad Bras Cienc 2001, 73, 525.
28. Wang, X.; Ma, J.; Wang, Y.; Binglin, H. Biomaterials 2001, 22, 2247.
29. Liu, Q.; de Wijn, J. R.; van Blitterswijk, C. A. J Biomed Mater Res 1998, 40, 257.
30. Murugan, R.; Ramakrishna, S. Acta Biomater 2006, 2, 201.